# Microwave Synthesis of Molybdenum Disulfide Nanoparticles using Response Surface Methodology for Tribological Application

**Thachnatharen Nagarajan**
National Defence University of Malaysia
**Mohammad Khalid** ( khalids@sunway.edu.my )
Sunway University
**Nanthini Sridewi**
National Defence University of Malaysia
**Priyanka Jagadish**
Sunway University
**Rashmi Walvekar**
Xiamen University Malaysia

**Article**

**Keywords:** Microwave synthesis, optimisation, MoS2 nanoparticles, nanolubricants, tribology

**Posted Date:** April 18th, 2022

**DOI:** https://doi.org/10.21203/rs.3.rs-1548749/v1

# Abstract

We used Response Surface Methodology (RSM) based on the Central Composite Design (CCD) model to optimise the synthesis time and temperature of the $MoS_2$ nanoparticles using the flexiWAVE microwave. Furthermore, the synthesised $MoS_2$ nanoparticles were used in SAE 20W50 diesel engine oil to study the tribological properties according to ASTM standard using a four-ball tribotester. The optimisation result shows synthesis temperature and time for the $MoS_2$ nanoparticles in the microwave were 200°C and 15 minutes, respectively, with a COF and average wear scar reaction of 0.0849 and 0.0852. The difference between the experimental and predicted values was minimal (1.88% (COF) and 3.40% (WSD)), which is similar to the DOE model.


# Introduction

An enormous amount of energy is used up in overcoming the friction of moving objects. As a result, friction-related wear and heat can cause damage to the contact surface, material fatigue, unnecessary mechanical energy losses, noise emissions, and degraded machine efficiency [1]. Friction and wear are two fundamental causes of the breakdown of engineering parts in various structures, such as gears and valves. The price of machinery, fitting and maintenance due to frictional defects, wear and tear put immense burdens on the nation's economy. Approximately 1/3 of fuel is utilised in passenger vehicles to subdue friction in engines, transmissions, and braking [2]. A decrease in energy usage can be accomplished mainly by enhancing the tribological properties of system surfaces. The specifications for improved lubricants are increasingly challenging due to their properties' usability across a broader temperature range, higher loads, higher speed, improved reliability and service life.

Military armoured vehicles with diesel-based engines experience massive heat generation and pressure due to their extensive driving in uneven terrains with bulky equipment. In order to ensure the mechanical parts are working efficiently and to increase the service life of the vehicle's engine, diesel-based engine oil must manage friction effectively and minimise wear for engine mechanical components [3].

The anti-friction additive is critical in the tribology of diesel-based engine oil, especially for military vehicles with rapidly evolving mechanical equipment. As a result, the load on a heavy-duty vehicle engine per unit mass increases, making it difficult for traditional lubricant additives to meet the demands of extreme operating conditions in modern diesel engine components [4, 5]. Therefore, developing new and effective friction-resistant plus high-bearing lubricant additives is critical for meeting the demands of powerful machinery in extreme working conditions.

One of the 21st century's main scientific challenges is producing new lubricants that satisfy evolving criteria in various strategic fields, such as transportation, manufacturing, and defence. In recent years, researchers have established that nanotechnology can be the most innovative aspect of science in the twenty-first century [6]. Continuous advances in science and technology provide an outstanding forum for nanotechnology to evolve at a faster pace. As a result of development, researchers also discovered that

lubricants' tribological properties could be improved with the inclusion of nanoparticles, which would significantly decrease the coefficient of kinetic friction in operating devices [7, 8].

Several nanoparticles consist of two adjacent layered structures, bound by weak van der Waals force, responsible for lowering the shear strength and causing sliding or lubricating effects on the system's active adjacent layer structure [9, 10]. Furthermore, two-dimensional (2D) nanomaterials have a larger specific surface area than other nanomaterial surfaces, allowing them to cover a large surface area during absorption on a substrate exterior, removing kinetic friction between two contact surfaces [11].

Due to its physical and chemical stability in lubrication, molybdenum disulfide (MoS2) is currently regarded as a high-potential 2D transition metal chalcogenide. The material is chemically balanced, resistive to most acids, and immune to irradiation. It is both semiconductor and diamagnetic in its purest form. The lubricant rate is dependent on its crystalline lamella structure, where the sulphur lamellae are linked by a weak van der Waals interaction which reduces the fiction [12]. During sliding, the crystalline layers of $MoS_2$ would effectively slide and align parallel to the relative movement, which causes the lubrication effect. However, the powerful ionic bond between S and Mo makes the lamellar highly resistant to asperities' penetration [13]. Nanostructure research has also been on the rise in the last few years. For example, using $MoS_2$ nanocrystals for lubrication will produce a superlubricity framework (a coefficient of friction lower than 0.01) [11]. Several theories have been proposed for this phenomenon, which has also been observed in fullerene configurations and nanotubes, where nanostructures act as nano bearings in tribological contact, lowering the mechanism's COF significantly [8, 14]. For the synthesis of $MoS_2$ nanoparticles, various preparatory methodologies have been established, including high-temperature sulfurisation, thermal reduction, hydrothermal process, laser ablation, and even chemical vapour deposition (CVD) [15–18]. However, advanced microwave synthesis of $MoS_2$ nanoparticles has rarely been documented, and its use in the tribology field has not been published in the literature so far.

Hydrothermal and microwave synthesis techniques have been employed to synthesise MoS2 nanoparticles at comparatively larger yields. The hydrothermal method is frequently used due to the accessibility of the processing equipment, but it suffers from a lack of even heating. However, substances can also be heated rapidly in the microwave synthesis process, producing a consistent temperature ramp relative to traditional oven-based hydrothermal processes. Besides that, the reaction Teflon vessels are translucent to the microwave, and will ensure continuous heating throughout the reaction vessels. In addition, microwave gains from rapid and accelerated heating, high-temperature homogeneity, and selective heating over traditional methods [19]. The reactions primarily depend on their precursors' ability, including solvents, to consume microwave energy efficiently. The above findings confirm that the microwave synthesis technique is superior to the hydrothermal technique due to its uniform heating, low energy consumption, higher yield, and shorter synthesis. In some papers [20–22], traditional heating in the oven that takes approximately 24 hours is employed to synthesise the MoS2 nanosheets, whereas microwave synthesis takes less than 30 minutes.

The novelty of this experiment is to investigate the optimisation of microwave-assisted synthesis of MoS2 nanoparticles for the tribological application using a response surface methodology (RSM) approach with a central composite design (CCD) model under Design Expert (Stat-Ease). Most of the previous studies were carried out using a univariate approach where only one element is varied at a time, often resulting in missing experimental data. However, with RSM and the CCD model, this optimisation approach investigates a larger experimental domain. The two vital experimental parameters for synthesis, such as temperature and time, vary together, resulting in higher optimum values. The principle purpose of this study is to identify the optimum time and temperature needed to synthesise the $MoS_2$ via microwave, which gives the best tribological result in military-grade diesel-based engine oil. Overall, this research highlights the effects of microwave synthesised nanoparticles on the tribological criteria of engine oil.

## Result And Discussion

# 2.1 Design of experiments and analysis of variance (ANOVA)

CCD model with two experimental factors (synthesis temperature and time) was used to determine the outcome of these experimental components on the COF and average WSD of the nanolubricant. The design of experiments generated by the CCD model with varying synthesis conditions and the experimental values of COF and the average WSD of the nanolubricant is shown in Table 1. The following evaluation was carried to reach the precision of the model: ANOVA analysis (Tables 2 and 4), normality assessment (Figs. 1 and 7), regression analysis (Tables 3 and 5), and residual analysis (Figs. 4, 5, 6, 10, 11 and 12) for COF and average WSD. After adequate completion of the above experiments in the range of the required statistical limits, the model equation is established. The variations in the parameter of the COF and the average WSD in the input variables are graphically shown in Figs. 2, 3, 8, and 9for nanolubricants based on microwave synthesised MoS2.

Table 1
Experimental design and results

| | Factor 1 | Factor 2 | Response 1 | Response 2 |
|---|---|---|---|---|
| Run | Synthesis temperature (°C) | Synthesis time (minutes) | Coefficient of Friction (COF) | Average Wear Scar Diameter (WSD) ($mm^3$ /Nm) |
| 1 | 185 | 17.0711 | 0.0861 | 0.0857 |
| 2 | 170 | 15 | 0.0868 | 0.088 |
| 3 | 200 | 5 | 0.0932 | 0.092 |
| 4 | 206 | 10 | 0.0852 | 0.0853 |
| 5 | 185 | 10 | 0.0923 | 0.0877 |
| 6 | 185 | 10 | 0.0917 | 0.0877 |
| 7 | 164 | 10 | 0.0865 | 0.0877 |
| 8 | 200 | 15 | 0.0834 | 0.0825 |
| 9 | 185 | 10 | 0.0912 | 0.088 |
| 10 | 185 | 3 | 0.0934 | 0.091 |
| 11 | 185 | 10 | 0.092 | 0.0872 |
| 12 | 185 | 10 | 0.0908 | 0.0867 |

# 3.1.1 Effect of Microwave Synthesis Temperature and Time on COF

Table 2 displays the ANOVA study of the COF produced by nanolubricant with microwave synthesised $MoS_2$ nanoparticles. In the current study, the confidence level of the CCD model is maintained at 95%. The F value of the model for $MoS_2$ nanolubricants is 55.80, and the p-value < 0.0001 indicates that the applied model is significant with a marginal noise effect on the COD of nanolubricants. The F and p value's lack of fit was not significant, which indicates that the chosen CCD model fits well with the COF experimental data set.

Careful analysis of the F and p values reveals that factor B (time) has a more significant effect on the COF of the nanolubricants of $MoS_2$ than factor A (temperature). The F test also projects the importance of factor B (time) to nanolubricants. The statistical accuracy is also tested to ensure the model's predictive capacity, as seen in Table 3. The approximate $R^2$ values for COF for nanolubricants are 0.9789, and this suggests an adequate description of the real interaction between the different experimental

variables for the model. Adequate precision, a calculation of the signal-to-noise ratio, is observed to be 21.926 for nanolubricants, as seen in Table 3. These values confirm the precision of the formula is higher, as the ratio is higher than 4. This model can also be deployed to traverse the design space.

Table 2
ANOVA table for COF of MoS2 nanolubricants

| Source | Sum of Squares | Degrees of freedom (df) | Mean Square | F-Value | p-value Prob > F | Significance |
|---|---|---|---|---|---|---|
| **Model** | 1.329E-004 | 5 | 2.659E-005 | 55.80 | < 0.0001 | significant |
| **A-Temperature** | 8.626E-008 | 1 | 8.626E-008 | 0.18 | 0.6853 | - |
| **B-Time** | 4.639E-005 | 1 | 4.639E-005 | 97.35 | < 0.0001 | - |
| **AB** | 8.846E-006 | 1 | 8.846E-006 | 18.56 | 0.0050 | - |
| **A2** | 5.103E-005 | 1 | 5.103E-005 | 107.10 | < 0.0001 | - |
| **B2** | 4.741E-006 | 1 | 4.741E-006 | 9.95 | 0.0197 | - |
| **Residual** | 2.859E-006 | 6 | 4.765E-007 | - | - | - |
| **Lack of Fit** | 1.399E-006 | 2 | 6.995E-007 | 1.92 | 0.2608 | not significant |
| **Pure Error** | 1.460E-006 | 4 | 3.650E-007 | - | - | - |
| **Cor Total** | 1.358E-004 | 11 | - | - | - | - |

Table 3
Model summary of the quadratic model for COF

| | |
|---|---|
| **R-Squared** | **0.9789** |
| **Adjusted R-Squared** | 0.9614 |
| **Predicted R-Squared** | 0.7907 |
| **Adequate Precision** | 21.926 |

Figure 1 displays the standard probability graph of the COF for the nanolubricants of $MoS_2$. The standard probability graph examines the experimental normality outcomes and displays the predicted versus actual values for the configuration matrix. For the ANOVA analysis, the standard probability graph must be tested for the residual range that should be closest to the mean line. From Fig. 1, It is clear that the residual values are minimal and closely associated with the mean line displayed in the graph.

The experimental outcome of the COF for $MoS_2$ nanolubricants was fitted to a quadratic polynomial equation as shown in equations (2).

Coefficient of Friction (COF) = (0.092) + (-1.199E-004* A) + (-2.781E-003* B) + (-1.920E-003* AB) + (-2.805E-003* A2) + (-8.550E-004* $B^2$) **(2)**

Coefficient of Friction (COF) = (-0.37880) + (4.86057E-003* A) + (+ 4.86339E-003* B) +

(-2.55975E-005* AB) + (-1.24665E-005* AB) + (-1.24665E-005 $A^2$) + (-3.41981E-005 $B^2$) **(3)**

Where A = Temperature (°C), B = Time (minutes)

Figs. 2 and 3 display the 3D surface response and contour plots, representing the regression equation acquired from the developed model. This is utilised to analyse the relationship between the experimental parameters such as synthesis temperature and time and its corresponding optimum values to achieve the lowest COF using the nanolubricant $MoS_2$. In addition, the elliptical or saddle form of the contour plot determines the value of the relationship, and an elliptical or saddle plot can be achieved where there is ideal interaction with the independent variables [24]. Moreover, Figs. 2 and 3 illustrate graphically the relationship between synthesis temperature and time on the COF for $MoS_2$ nanolubricants. Both plots clearly show that as the time and temperature variables of the $MoS_2$ microwave synthesis increase, the COF of the nanolubricant decreases. The dark blue area represents the lowest COF of the nanolubricant. The dark blue area represents a large region of lowest frictional values (<0.08) at the time above 15 minutes and temperature around 200°C. The crystallinity of the $MoS_2$ nanoparticle improves as the microwave synthesis time and temperature increase. The nanoparticle's crystallinity is attributed to its mechanical strength and has improved tribological properties by reducing the COF of the nanolubricant based $MoS_2$.

Residual analysis was carried out due to the close approximation of the actual system. Residuals (*ri*) is extracted from the following regression:

*ri = yi observed − yi predicted* **(4)**

Where, *r* is residuals, *y* is response and *i* is observation.

Value of all residual observations used in the residual plot involving the residual vs. the predicted plot and the residual vs. the experimental run plot. Residual vs. predicted plot and residual vs. experimental run plot of the COF for $MoS_2$ nanolubricants are shown in the Figs. 4 and 5, respectively, which is the significant diagnosis for the model. In accordance with Draper and Smith [25], a linear relationship is normal in error terms. Our results have shown no defects, suggesting that errors obey the normal distribution and endorse the experimental model.

In addition, an irregular pattern of scattering is observed from the residual vs. the predicted plot in the figure. 4. Residuals are well proportioned in positive and negative residues within a gradient of -2 ≤ *ri* ≤ +2 (*ri* is actual residuals). Moreover, in the diagram, no trend matches the residual vs. experimental run plot. 6, which confirms that not all residues are associated with one and another as a consequence of time-related variables. The established model is appropriate, and no indication of any violation of the objectivity or the constant variance hypothesis. Figure 6 displays the predicted vs. actual COF results for MoS2 nanolubricants. The points are irregularly scattered along the 45-degree line and indicate the accuracy of the predicted data on the actual data. It remarks on the design, and results validate the excellent predictability.

# 3.1.2 ANOVA analysis of average WSD

The contact area's wear rate in the thin film lubrication regime is a critical parameter in tribological experiments, along with the COF used to select the required lubricant. The WSD investigation is considered one of the conventional methods of recognising the wear output of lubricating oil. The wear scars were created due to the spindle's sliding motion in a four-ball machine, and an image acquisition system was utilised to analyse and scale the WSD of each ball. Additionally, the average WSD of the fixed balls was determined using Eq. 5.

*WSD Mean (mm2) = [scar (1) diameter + scar (2) diameter + scar (3) diameter]/3* **(5)**

ANOVA study of the average WSD was performed using the same design methods to analyse the COF. The overview of analyses for nanolubricants is seen in Table 4 for the association of process parameters and F and p values. The temperature is a less critical parameter within the chosen confidence degree, while the time is a more significant parameter for nanolubricants when referring to the F value. According to Table 5, the approximate values of $R^2$ for the model developed for a particular rate of wear for $MoS_2$ nanolubricants is 0.9474, which is satisfactory. The modified $R^2$ values of 0.9174 are similar to the respective $R^2$ values that confirm the model's fair predictability within the parametric range domain. The regression equations obtained from the model and evaluated for normality (Fig. 7) are given in equations

6 and 7, respectively, for nanolubricants of $MoS_2$. The data plotted in Fig. 7 exhibit good behaviour as the residual data are very minute and closely associated with the mean line. Thus, the data shows a good agreement with the model.

Average Wear Scar Diameter (WSD)= (+ 0.088) + (-5.095E-004* A) + (-2.022E-003* B) + (-2.580E-003* AB) + (-5.390E-004* A2) **(6)**

Average Wear Scar Diameter (WSD)= (-0.047524) +(+ 1.19638E-003* A) + (+ 5.95843E-003* B) + ( -3.43938E-005* AB) + ( -2.39569E-006* A2) **(7)**

Where A = Temperature (°C), B = Time (minutes)

Table 4
ANOVA table for average WSD of $MoS_2$ nanolubricants

| Source | Sum of Squares | Degrees of freedom (df) | Mean Square | F-Value | p-value Prob > F | Significance |
|---|---|---|---|---|---|---|
| **Model** | 6.339E-005 | 4 | 1.585E-005 | 31.53 | 0.0001 | significant |
| **A-Temperature** | 1.584E-006 | 1 | 1.584E-006 | 3.15 | 0.1191 | - |
| **B-Time** | 2.496E-005 | 1 | 2.496E-005 | 49.66 | 0.0002 | - |
| **AB** | 1.641E-005 | 1 | 1.641E-005 | 32.66 | 0.0007 | - |
| **A2** | 1.955E-006 | 1 | 1.955E-006 | 3.89 | 0.0892 | - |
| **Residual** | 3.518E-006 | 7 | 5.026E-007 | - | - | - |
| **Lack of Fit** | 2.466E-006 | 3 | 8.220E-007 | 3.13 | 0.1499 | not significant |
| **Pure Error** | 1.052E-006 | 4 | 2.630E-007 | - | - | - |
| **Cor Total** | 6.691E-005 | 11 | - | - | - | - |

Table 5
Model summary of the quadratic model for average WSD

| | |
|---|---|
| **R-Squared** | **0.9474** |
| **Adjusted R-Squared** | 0.9174 |
| **Predicted R-Squared** | 0.7367 |
| **Adequate Precision** | 20.112 |

Interaction between various times and temperatures on average WSD for $MoS_2$ nanolubricants was examined and demonstrated using 3-D response surface and contour plots. From the quadratic model mentioned earlier (Eqs. (6 and 7)), the surface response and contour charts show the interaction effect of the average WSD of the $MoS_2$ nanolubricants in Figs. 8 and 9. The selection of the required time and temperature for the advanced microwave synthesis of $MoS_2$ is crucial in this analysis to determine the average WSD for nanolubricants. It is clear from Figs. 9 and 10 the increase in synthesis time and temperature contributes to lower average WSD $MoS_2$ nanolubricants.

It was found that when the $MoS_2$ synthesised at higher temperatures (~ 200°C) and duration (~ 15 minutes), it resulted in the lowest average WSD of ~ 0.0830 $mm^2$. This shows a linear relationship between time and temperature and average WSD; as time and temperature rise, the average WSD decreases but above 15 minutes of synthesis time, the average WSD increases. From the data shown above, it can be inferred that when the precursors of $MoS_2$ are subjected to optimum microwave synthesis time and temperature, the average WSD during tribological studies is decreased. This effect arises when well-formed $MoS_2$ with higher crystallinity has a lower WSD due to the formation of tribofilm between the contact surface [26].

Figure 10 represents a plot for residual vs. predicted values typically used to define or validate the presumption of constant variance. The graph shows a strong constant variance, and the values are well spaced and randomly distributed along the line outcomes; therefore, the model correctly matches the variances. Figure 11 displays the residual versus run map, where the values are uniformly distributed, and most of the values are within the positive range. There are no outliers and extreme points in the chart, which means that the model fit strongly aligns with the run. Figure 12 provides a contrast between the expected and the actual values, showing that they strongly align with the response result (average WSD). The plot shows that more than 90% of the actual values fit the predicted values.

# 3.2 Characterisation of $MoS_2$

**3.2.1** Field Emission Scanning Electron Microscope (FESEM) and Energy Dispersive X-Ray Spectroscopy (EDS) of optimised $MoS_2$ nanoparticle

FESEM images of the $MoS_2$ nanoparticles confirm the layered lamellar structure of $MoS_2$ nanoparticles at two different magnifications from Fig. 14 (a) and (b). Figure 14 (c) and (d) depict the EDS analysis of $MoS_2$ nanoparticles based on their atomic and weight percentage reveals the quantitative surface analysis of EDS performed in terms of atomic and weight percentage of element on the $MoS_2$ nanoparticles reveals the existence of sulfur and molybdenum.

# 3.2.2 X-Ray diffraction of optimised $MoS_2$ nanoparticle

Figure 15 shows the XRD diffraction peaks of $MoS_2$ at 2 = 14.5°, 33.0°, 39.3°, 58.5°, and 69.7°, which can be indexed as the (002), (100), (103), (110), and (201) peaks of pure hexagonal $MoS_2$ phase (JCPDS card

no.371492), which are in accordance with previous studies[27, 28]. Peak broadening is seen, implying that the crystalline size is very small. For (100) and (103) XRD peaks, the intensity variation in between the reference pattern in the JCPD card and the synthesised sample is due to differences in texture of crystallite size difference and the size of the scattering domains. There are no other impurities peaks or separate phases in the XRD patterns, indicating that the crystal structure is pure $MoS_2$ nanosheets.

According to the characterisation of the $MoS_2$ nanoparticle, the nano-lubricants' improved tribological properties are due to adequate exfoliation force at the contacting surface and the configuration of tribo-films in between the contact exterior. A sufficient exfoliation pressure causes the deformation of nanoparticles required for the sliding effect, which promotes tribological properties. This exfoliation and deformation of nanoparticles result in the occupancy of MoS2 nanoparticles in the asperity contacts of the ball bearing contact surfaces in the four-ball tribotester, resulting in the formation of tribo-film[29]. This clearly shows that the laminar tribo-film is responsible for reducing friction and anti-wear properties of nano-lubricants, rather than tribo-chemical reactions, which involve $MoS_2$ nanoparticles[30, 31].

## 3.3 Optimisation of time and temperature for $MoS_2$ microwave synthesis for tribological application

COF and average WSD are the two key characteristics of the tribology, the interpretation of which is described in the preceding parts. Beyond the effectiveness of nanoparticle additives in lubricants, the synthesis approach with optimal temperature and time for reactions to favourable responses is necessary. As an outcome, a multiple objective optimisation methods had been developed and integrated into Design of Expert (DOE) software with the aid of desirability features. The optimised synthesising time and temperature obtained from DOE software were validated to verify the expected and experimental values discrepancy. The optimisation procedure was carried out at rotating speed, applied load, time, and temperature of 12000 rpm, 392.5N, 3600 sec, and 75°C, respectively, as per ASTM standard. According to Fig. 13, the optimum synthesis time and temperature of $MoS_2$ through the microwave for best tribological performance is 199.958°C and 14.8118 minutes with 1.000 desirability in the SAE 20W50 diesel engine oil. The predicted COF and average WSD are 0.0833 and 0.0823, respectively.

In this optimised synthesis time and temperature of the $MoS_2$ nanoparticles, real-time analyses were carried to calculate the lowest COF and the average WSD of the nanolubricants. The model outcomes for COF and average WSD are confirmed with in-situ experimental results at an optimal synthesis time and temperature of the $MoS_2$ nanoparticles and are shown in Table 8. As predicted, the experimental findings have shown a reduction in friction and anti-wear characteristics (Table 8) with the inclusion of $MoS_2$ nanoparticles. The experimental result for COF and average WSD with the error percentage values is 0.0849 (1.88% error) and 0.0852 (3.40% error) for $MoS_2$ nanolubricants. The error percentage values have demonstrated a proximity prediction between the predicted and actual properties. These error values explicitly show the model's accuracy in relation to the domain of experimental operating conditions.

Table 6
Model validation for MoS2 nanolubricants

| Response | Predicted | Experimental | % Error |
|---|---|---|---|
| **Coefficient of Friction (COF)** | 0.0833 | 0.0849 | 1.88 |
| **Average (WSD)** | 0.0823 | 0.0852 | 3.40 |

## Conclusions

The statistical study of the lowest COF and WSD using the parameter of synthesising time and temperature of the $MoS_2$ nanoparticles through Design of Expert (DOE) was successfully completed. DOE analysis based on Response Surface Method (RSM) using Central Composite Design (CCD) and ANOVA has proven as a promising method for evaluating important parameters and maximising operational factors related to the tribological properties of $MoS_2$ nanolubricants. Study of ANOVA, normality assessment, regression analysis, residual analysis, surface response plots, and contour plots demonstrated a close relationship between the experimental outcomes and the model's predicted values.

Optimised temperature and time generated were 199.958°C and 14.8118 minutes with 1.000 desirability conditions predicting a COF and an average WSD response of 0.0833 and 0.0823, respectively. The R-squared values of each analysis were 0.9789 (COF) and 0.9474 (WSD), which suggests a strong correlation with the model fit. The experimental effect of the COF and the average WSD for the optimised synthesising time and temperature of the $MoS_2$ nanoparticles is 0.0849 (COF) and 0.0852 (WSD), consistent with the predicted values of 0.0833 and 0.0823, respectively. The discrepancy between the experimental and the expected values is 1.88% (COF) and 3.40% (WSD), which indicates that the experimental configuration of the DOE is validated accurately.

## Materials And Methods

# 3.2 Materials

All the chemical substances used in the investigation were of analytical grade and were not further purified. The chemicals used for the preparation of MoS2, such as ammonium molybdate tetrahydrate ((NH4)6Mo7O24.4H2O) and thiourea (SC(NH2)2), were purchased from Fisher and R&M Chemicals. The base oil used was the SAE 20W50 diesel engine oil.

# 3.3 Preparation of MoS2 Nanoparticles using Microwave

All the chemical reagents were measured using an analytical balance with the precision of ± 0.1 mg (Mettler Toledo, Switzerland). 1 mmol of ammonium molybdate tetrahydrate ((NH4)6Mo7O24.4H2O) and 30 mmol thiourea (SC(NH2)2) were dissolved in 35 mL of deionised water. The solution was stirred for 20 minutes at room temperature. The obtained homogeneous solution was transferred into a microwave advanced flexible microwave synthesis platform (flexiWAVE Milestone, Italy) Teflon vessel. Twelve

different samples of $MoS_2$ were synthesised according to the time and temperature combinations generated by the Design-Expert version 9 (Stat-Ease) software, as shown in Table 1. After the reaction mixtures had cooled to room temperature, the samples were centrifuged and washed with deionised water and ethanol multiple times and then dried in a vacuum oven at 70°C for 12 hours.

Table 7
Parameter ranges selected for the study using CCD

| Coded name | Variable name | Type | Parameter range | Parameter unit |
|---|---|---|---|---|
| A | Temperature | Continuous | Level 1 / low 170<br>Level 2 / high 200 | °C |
| B | Time | Continuous | Level 1 / low 5<br>Level 2 / high 15 | minutes |

# 3.4 Experimental Design and Statistical Analysis

Theoretic assumptions based on scientific findings are the core of the beneficial analysis. There are two fundamental areas of interest in scientific experimentation: the design of the experiment and the statistical analysis of the results. The Design of Experiments (DOE) aims to evaluate the important parameters for understanding variance in the process [23]. DOE also tries to consider how influential forces are interfering with the system.

In this study, the Response Surface Method (RSM) is applied to analyse the effect of input parameters on the response parameters. RSM is a set of mathematical and computational techniques helpful in modelling and evaluating problems in which various variables influence the solution of interest. If all input parameters depict quantitative variables, the response could be interpreted as functional stages and variables shown by Eq. 1.

$$Y = f(X1u, X2u, \ldots, Xiu) + Eu \quad (1)$$

where $u = 1, 2, \ldots, N$ represents $N$ observations in the empirical studies, and $Xiu$ shows the degree of *ith* Factor of *uth* Observation. Function $f$ is considered the function of response. The residual $Eu$ measures the experimental error of the $u^{th}$ measurements.

The RSM algorithm employs a factorial design, with main effects defined as the difference in response caused by a change in the reasoned factor while all other factors remain constant. A polynomial regression modifies the experimental results to the above equation, and the standard statistics can be used to determine the model's fitness. The analysis of variance (ANOVA) must be conducted to assess the significance of the established model and the importance of the specific coefficients model. The ANOVA describes the critical consequences and relationships, the regression coefficients, and the *p*-value. The F-value and *p*-value of the ANOVA study facilitate assessing the results, which is that the factors and interactions are statistically important. The lower the *p*-value, the lower the probability of an error by

declining the null hypothesis. It is also proposed that the *p*-value be less than 0.05, making the model meaningful at 95% confidence level. The ANOVA was also performed to explain the validity and adequacy of the regression model. In the interest to determine the fitness of the experiment, the value of the correlation coefficient ($R^2$) was used, and the statistical significance of the model equation was tested using the F test.

This research uses RSM to optimise two experimental parameters (1) synthesis temperature and (2) synthesis time required for the microwave synthesis of MoS2 on the tribological activity of nanolubricants tested using a four-ball tribotester. The coefficient of friction and specific rate of wear is used as response factors. The program Design-Expert version 9 (Stat-Ease) is used for research, and the tests are formulated using the Central Composite Design (CCD) model. Based on the CCD configuration, 12 experimental runs with different times and temperatures synthesised $MoS_2$ nanoparticles using the microwave were generated.

# 2.4 Formulation of Nanolubricant

The constant 0.05 wt.% of the obtained MoS2 nanoparticles were dispersed in 100ml of SAE 20W50 military-grade diesel engine oil with the help of homogeniser at 7000 rpm for 10 minutes. The samples were sonicator using bath sonication for 30 minutes to assure that the nanoparticles were uniformly dispersed in the base oil. The formulated nanolubricants have shown high stability for more than a week.

# 2.5 Tribological study

The Coefficient of Friction (COF) and Wear Scar Diameter (WSD) of the nanolubricant were examined by a four-ball tribotester (DUCOM). Tribological tests were performed by submerging steel balls in nanolubricants as the rotating ball in contact with the other three ball in the ball pot. The metal ball bearings employed in the tests are equivalent to 12.7 mm in diameter. The mechanical details regarding the properties of the metal ball bearings utilised as seen in Table 2. Before the experiment, the steel balls and other equipment had been cleaned with ethanol and dried to deter impurities. All testing parameters: rotating speed, applied load, time, and temperature, were 12000 rpm, 392.5N, 3600 sec, and 75°C, respectively, as per ASTM standard. Figure 1 shows the experimental configuration of the four-ball tribotesters schematic drawing. The main data processor connected to the tribotester recorded the nanolubricant COF, and the wear scar's diameter was measured using image acquisition devices.

Table 8
Mechanical details of the metal ball bearing

| Properties | Ball bearing |
|---|---|
| Material | Carbon-chromium steel |
| Hardness (*H*), HRC | 1 |
| Density (ρ), gm/cm$^3$ | 7.79 |
| Surface roughness (Ra), μm | 0.022 |

# 2.6 Characterisation of Nanoparticles

The characterisation of $MoS_2$ nanoparticles for particle morphology and size distributions was confirmed using a Field Emission Scanning Electron Microscope (FESEM, HITACHI SU6600) and Energy Dispersive Spectroscopy (EDS, HORIBA-EMAX) for nanoparticle composition. X-ray Diffractometer was used to collect XRD data. A sample of $MoS_2$ nanoparticles was scanned from 20 to 80 degrees at a step size of 1 degree/min. The size of the divergence slit is 0.9570 degrees. Copper material was used to generate X-rays with a wavelength (K alpha) of 1.54 angstroms. X-rays were filtered through Ni using an operational voltage of 45 kV and a current of 27 mA.

## Declarations

# Acknowledgement

The authors gratefully acknowledge Sunway University for awarding Individual Research Grant (GRTIN-IRG-03-2021). Also, the authors wish to thank the Research and Innovation Management Centre of National Defence University of Malaysia for providing financial support for the research.

### Availability of Data and Materials

All data generated or analysed during this study are included in this published article. Additional data is available from the corresponding author on request.

## References

1. Tung, S.C. and M.L. McMillan, *Automotive tribology overview of current advances and challenges for the future*. Tribology International, 2004. **37**(7): p. 517–536.
2. Holmberg, K., P. Andersson, and A. Erdemir, *Global energy consumption due to friction in passenger cars*. Tribology international, 2012. **47**: p. 221–234.
3. Xu, X., et al., *Study on tribology performance of diesel engine oil using SRV4 tribometer*. Tribology Online, 2015. **10**(2): p. 172–176.
4. Johnson, D.W., M. Bachus, and J.E. Hils, Interaction between lubricants containing phosphate ester additives and stainless steels. Lubricants, 2013. **1**(2): p. 48–60.
5. Agarwal, R.K., *Recent Progress in Some Aircraft Technologies*. 2016: BoD–Books on Demand.
6. Wu, Y., W. Tsui, and T. Liu, *Experimental analysis of tribological properties of lubricating oils with nanoparticle additives*. Wear, 2007. **262**(7–8): p. 819–825.
7. Rosentsveig, R., et al., *Fullerene-like MoS 2 nanoparticles and their tribological behavior*. Tribology Letters, 2009. **36**(2): p. 175–182.
8. Kalin, M., J. Kogovšek, and M. Remškar, *Mechanisms and improvements in the friction and wear behavior using MoS2 nanotubes as potential oil additives*. Wear, 2012. **280**: p. 36–45.

9. Hilton, M.R., et al., *Structural and tribological studies of MoS2 solid lubricant films having tailored metal-multilayer nanostructures*. Surface and Coatings Technology, 1992. **53**(1): p. 13–23.
10. He, X., et al., *α-Zirconium phosphate nanoplatelets as lubricant additives*. Colloids and Surfaces A: Physicochemical and Engineering Aspects, 2014. **452**: p. 32–38.
11. Vattikuti, S. and C. Byon, *Synthesis and characterisation of molybdenum disulfide nanoflowers and nanosheets: nanotribology*. Journal of Nanomaterials, 2015. **2015**.
12. Berman, D., A. Erdemir, and A.V. Sumant, *Graphene: a new emerging lubricant*. Materials Today, 2014. **17**(1): p. 31–42.
13. Dallavalle, M., N. Sändig, and F. Zerbetto, *Stability, dynamics, and lubrication of MoS2 platelets and nanotubes*. Langmuir, 2012. **28**(19): p. 7393–7400.
14. Uzcanga, I., et al., *Sonochemical preparation of MoS2 in aqueous solution: replication of the cavitation bubbles in an inorganic material morphology*. Chemistry of materials, 2005. **17**(14): p. 3575–3577.
15. Li, X.L. and Y.D. Li, *Formation of MoS2 inorganic fullerenes (IFs) by the reaction of MoO3 nanobelts and S*. Chemistry–A European Journal, 2003. **9**(12): p. 2726–2731.
16. Rapoport, L., N. Fleischer, and R. Tenne, *Applications of WS 2 (MoS 2) inorganic nanotubes and fullerene-like nanoparticles for solid lubrication and for structural nanocomposites*. Journal of Materials Chemistry, 2005. **15**(18): p. 1782–1788.
17. Tang, G., et al., *Hydrothermal synthesis and characterisation of novel flowerlike MoS2 hollow microspheres*. Materials Letters, 2013. **100**: p. 15–18.
18. Gawande, M.B., et al., *Microwave-assisted chemistry: synthetic applications for rapid assembly of nanomaterials and organics*. Accounts of chemical research, 2014. **47**(4): p. 1338–1348.
19. Li, W.-J., et al., *Hydrothermal synthesis of MoS2 nanowires*. Journal of Crystal Growth, 2003. **250**(3–4): p. 418–422.
20. Lin, H., et al., *Hydrothermal synthesis and characterisation of MoS2 nanorods*. Materials letters, 2010. **64**(15): p. 1748–1750.
21. Peng, Y., et al., *Hydrothermal synthesis of MoS2 and its pressure-related crystallisation*. Journal of Solid State Chemistry, 2001. **159**(1): p. 170–173.
22. Muralikrishna, S., et al., *Hydrothermal synthesis of 2D MoS 2 nanosheets for electrocatalytic hydrogen evolution reaction*. RSC advances, 2015. **5**(109): p. 89389–89396.
23. Cho, M. and H.-J. Choi, *Optimisation of surface texturing for contact between steel and ultrahigh molecular weight polyethylene under boundary lubrication*. Tribology Letters, 2014. **56**(3): p. 409–422.
24. Danish, M., S.M. Yahya, and B.B. Saha, *Modelling and optimisation of thermophysical properties of aqueous titania nanofluid using response surface methodology*. Journal of Thermal Analysis and Calorimetry, 2020. **139**(5): p. 3051–3063.
25. Draper, N.R. and H. Smith, *Applied regression analysis*. Vol. 326. 1998: John Wiley & Sons.

26. Vaitkunaite, G., et al., *MoS2 tribofilm distribution from low viscosity lubricants and its effect on friction*. Tribology International, 2020. **151**: p. 106531.
27. Solomon, G., et al., *Ag2S/MoS2 nanocomposites anchored on reduced graphene oxide: fast interfacial charge transfer for hydrogen evolution reaction*. ACS applied materials & interfaces, 2019. **11**(25): p. 22380–22389.
28. Park, S.-K., et al., *A simple l-cysteine-assisted method for the growth of MoS 2 nanosheets on carbon nanotubes for high-performance lithium ion batteries*. Dalton Transactions, 2013. **42**(7): p. 2399–2405.
29. Frene, J., et al., *Hydrodynamic lubrication: bearings and thrust bearings*. 1997: Elsevier.
30. Ing, T.C., et al., *Tribological behaviour of refined bleached and deodorised palm olein in different loads using a four-ball tribotester*. Scientia Iranica, 2012. **19**(6): p. 1487–1492.
31. Hu, E., et al., *The role of soot particles in the tribological behavior of engine lubricating oils*. Wear, 2013. **304**(1–2): p. 152–161.

# Figures

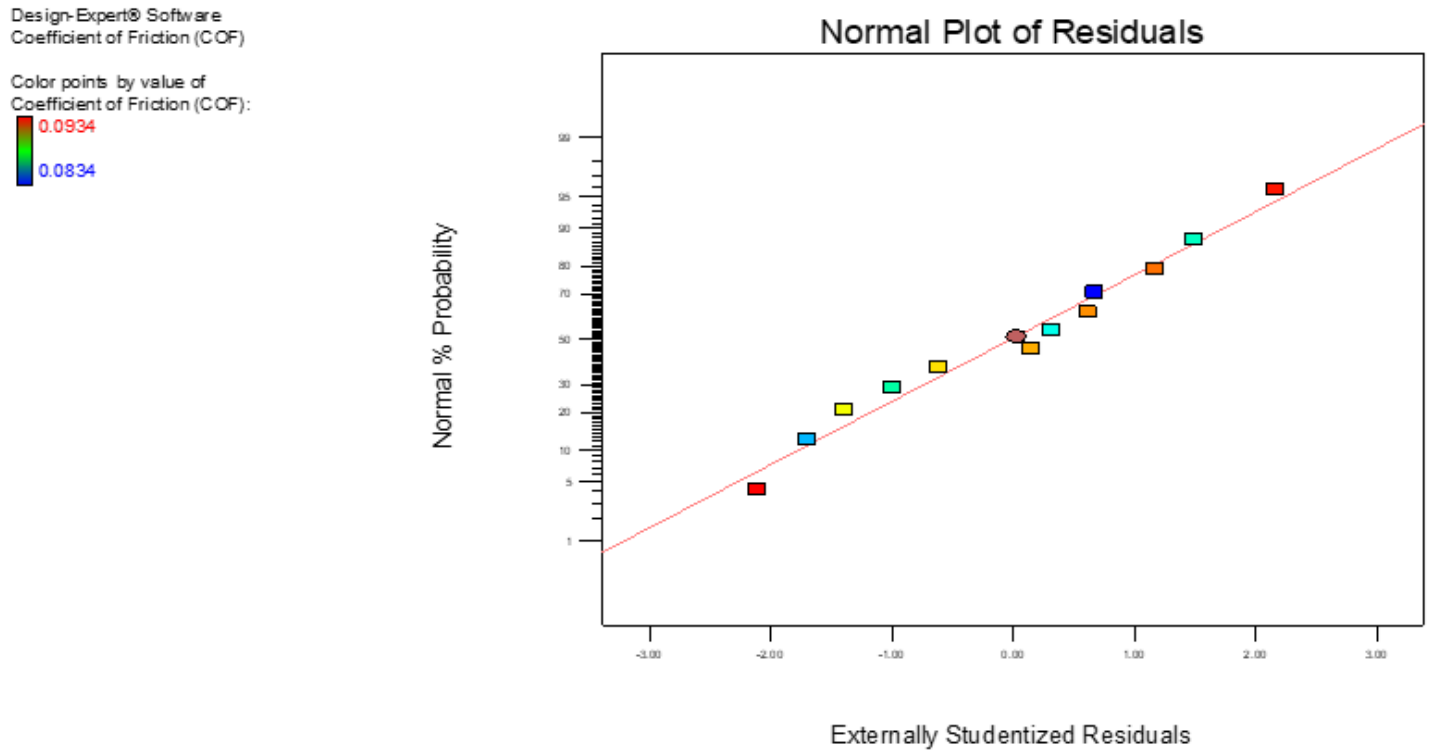


**Figure 1**

Normal probability plot of COF for $MoS_2$ nanolubricants

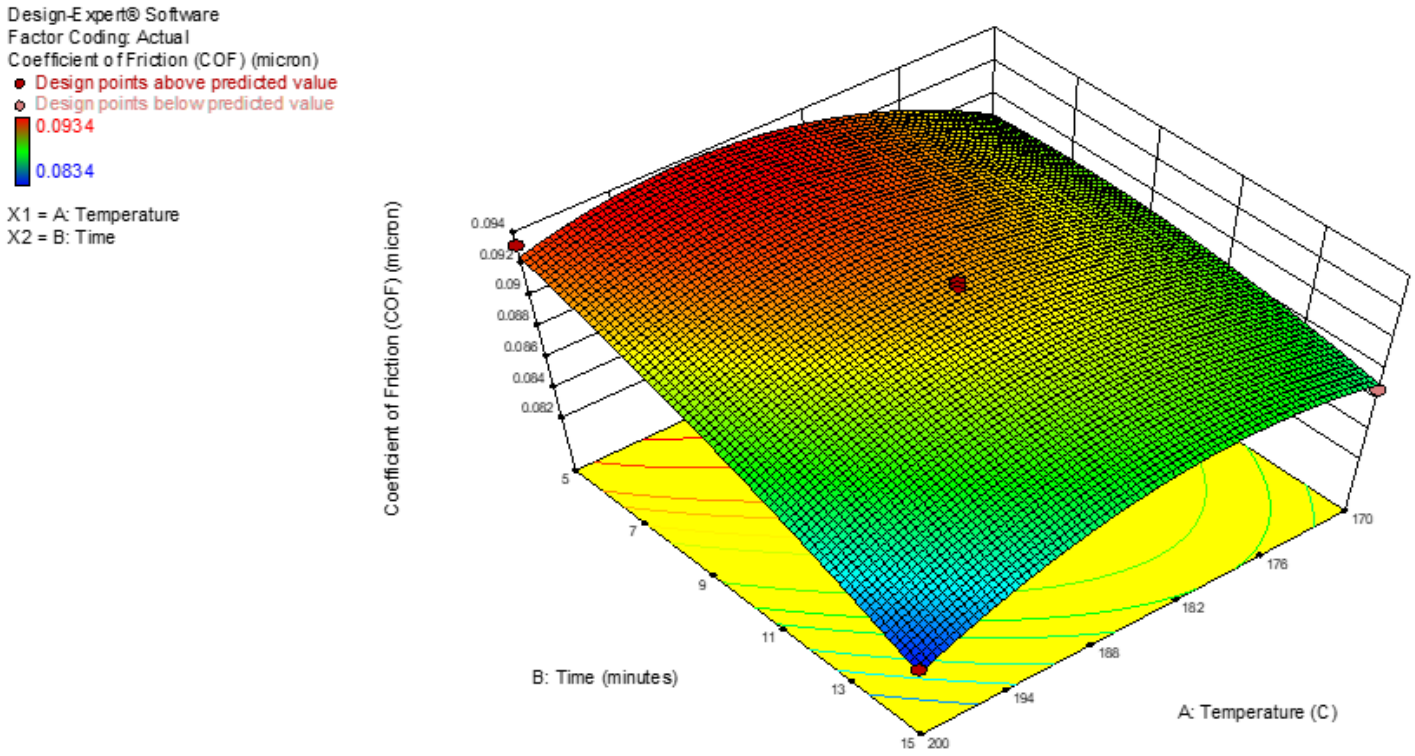


## Figure 2

A 3D interaction plot of COF for $MoS_2$ nanolubricants

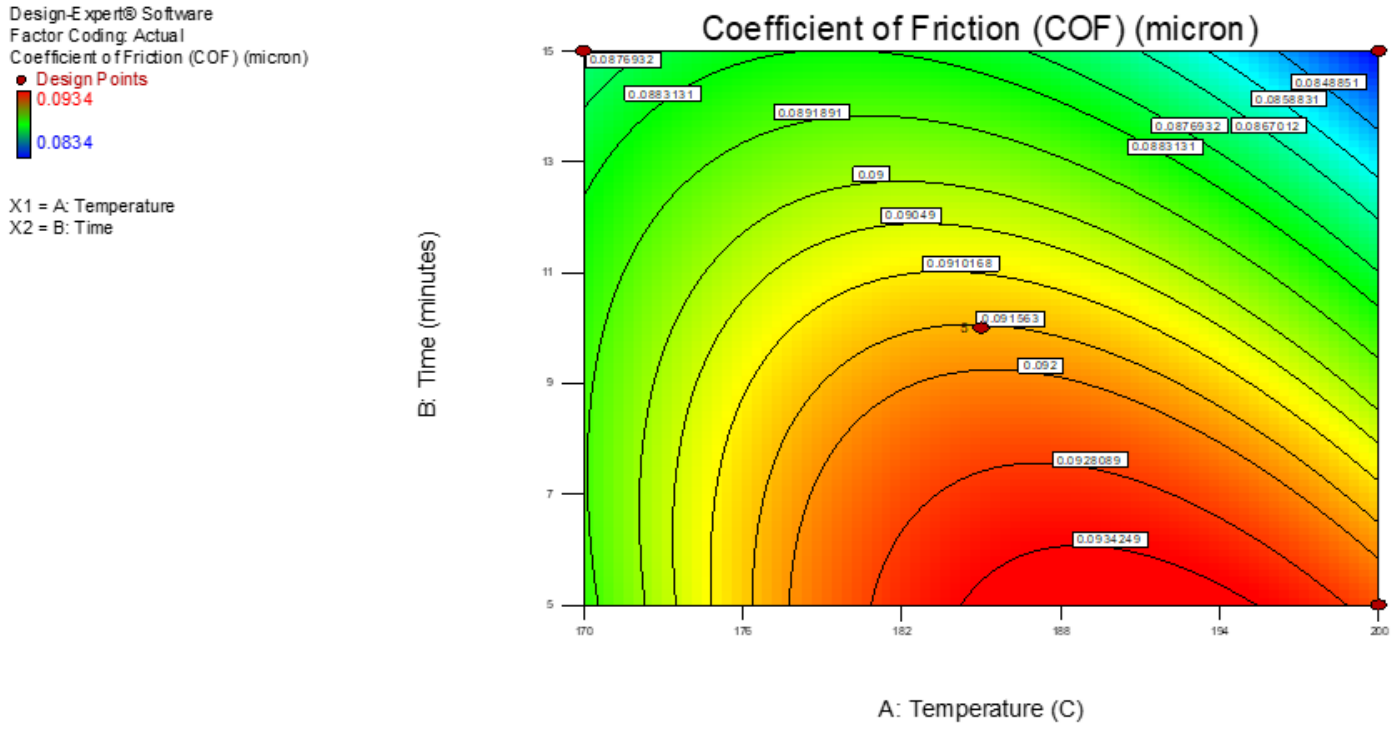


## Figure 3

A contour interaction plot of COF for $MoS_2$ nanolubricants

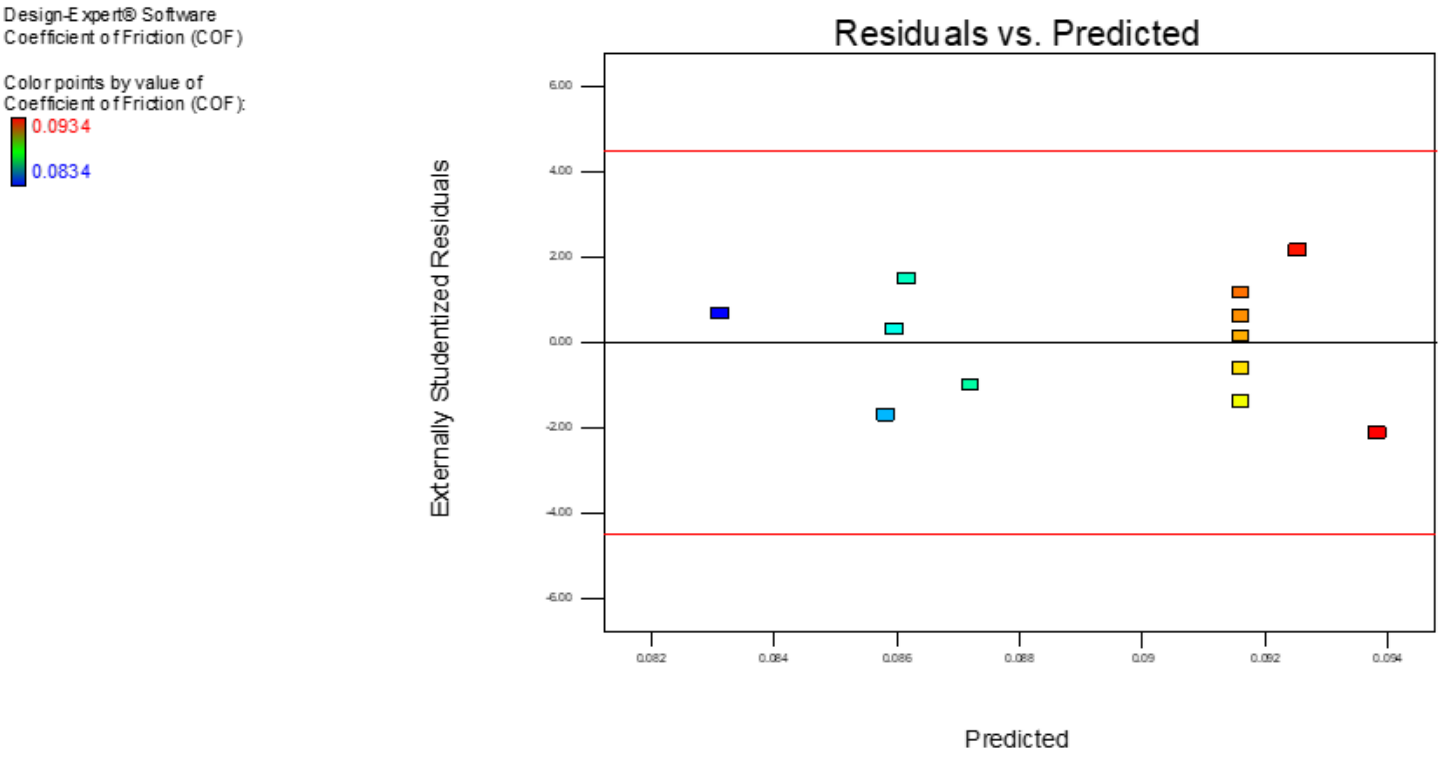


**Figure 4**

Residuals vs. predicted of COF for $MoS_2$ nanolubricants

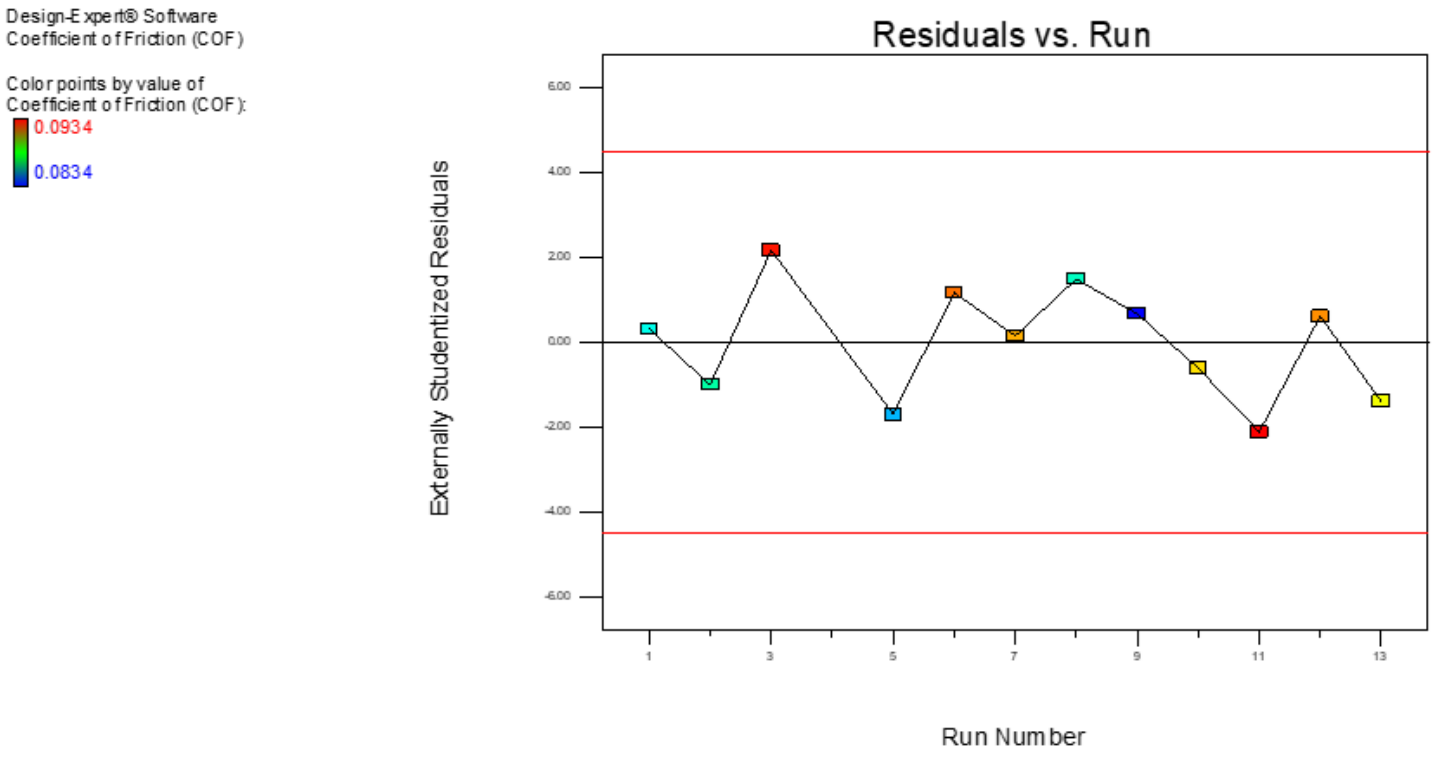


## Figure 5

Residuals vs. Experimental run of COF for MoS2 nanolubricants

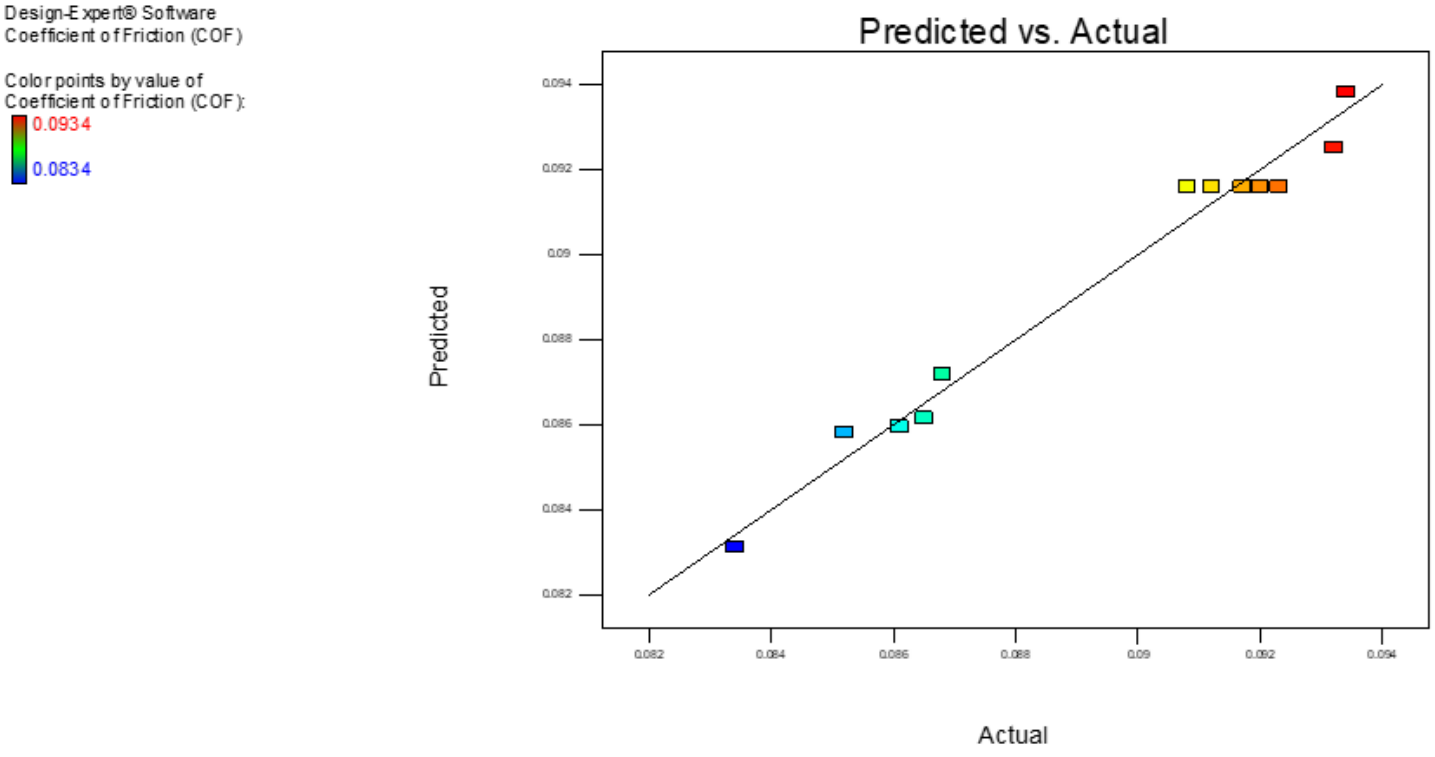

## Figure 6

Predicted vs. Actual of COF for MoS2 nanolubricants

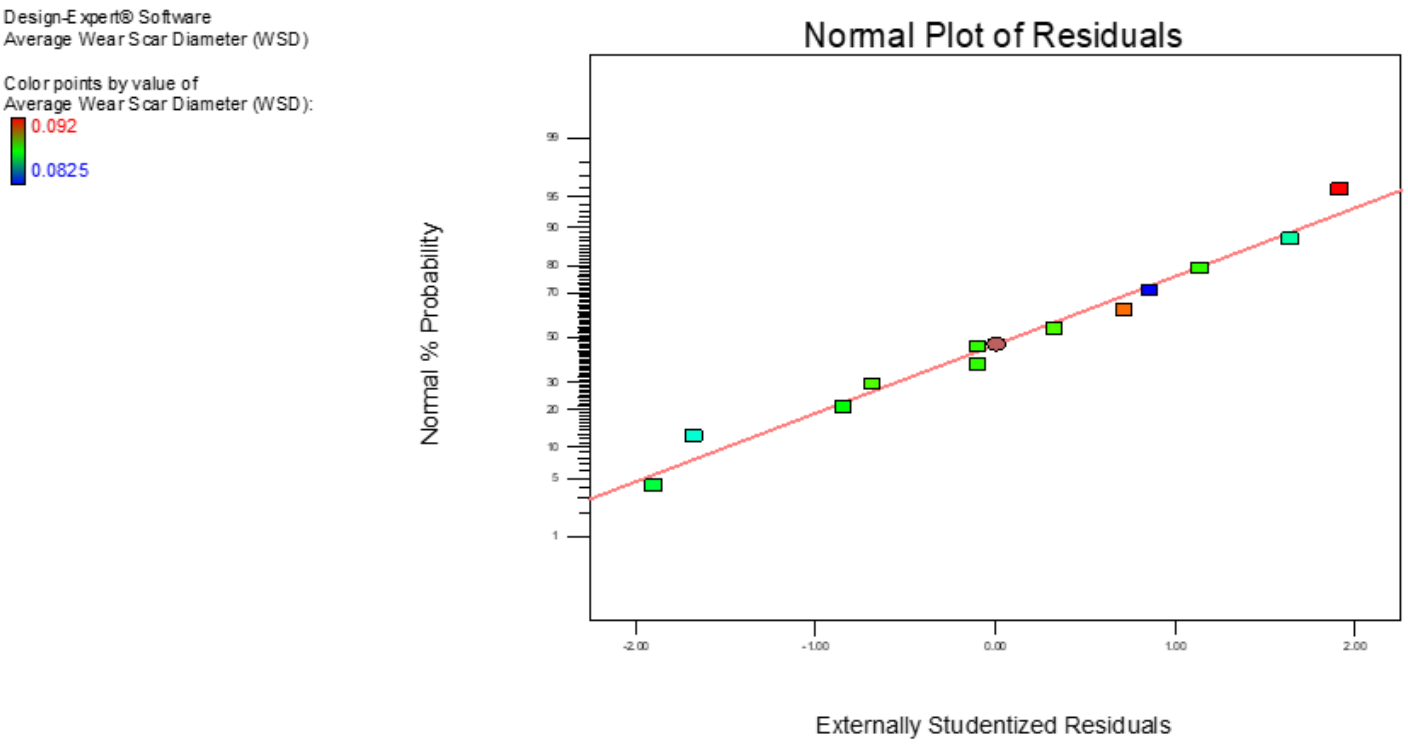


## Figure 7

Normal probability plot of average WSD for MoS2 nanolubricants

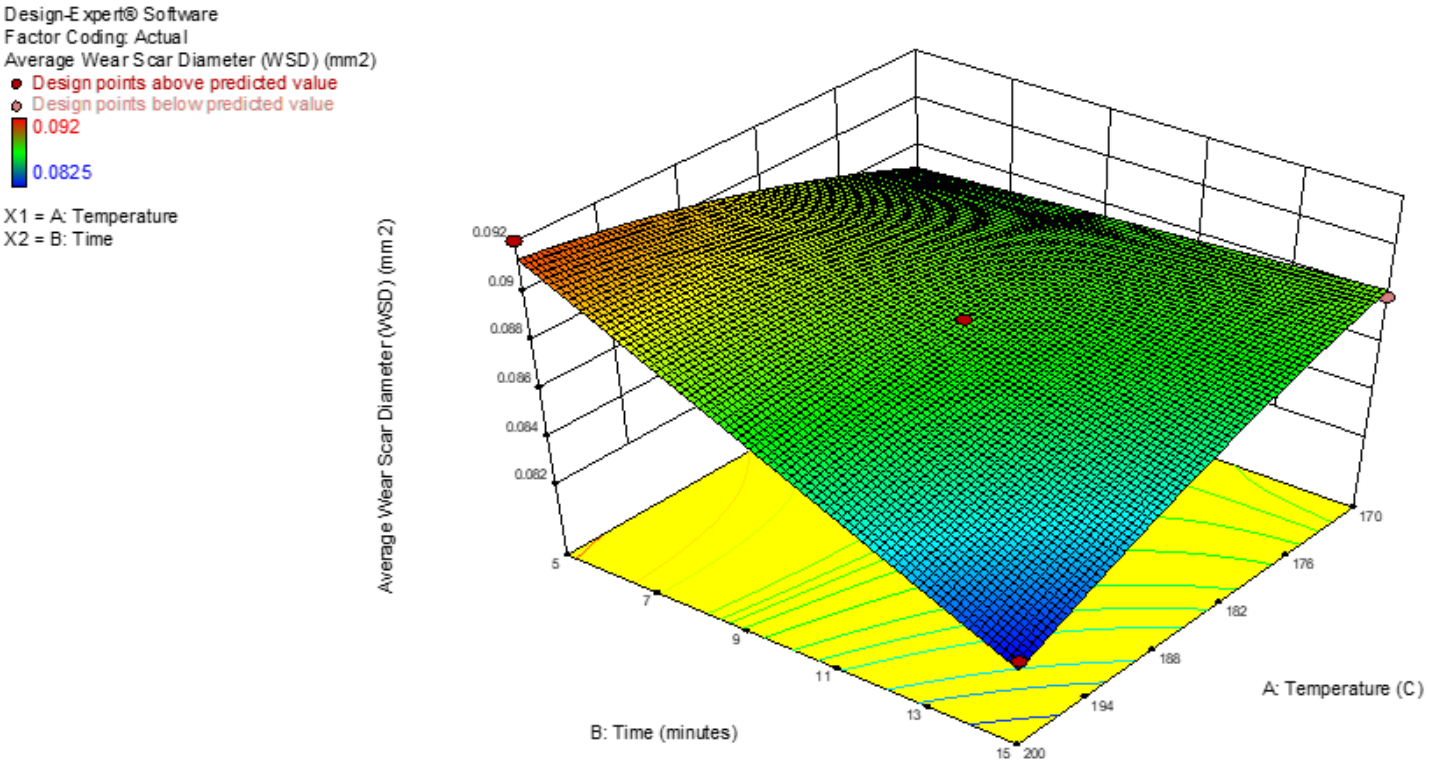


## Figure 8

A 3D interaction plot of average WSD for MoS2 nanolubricants

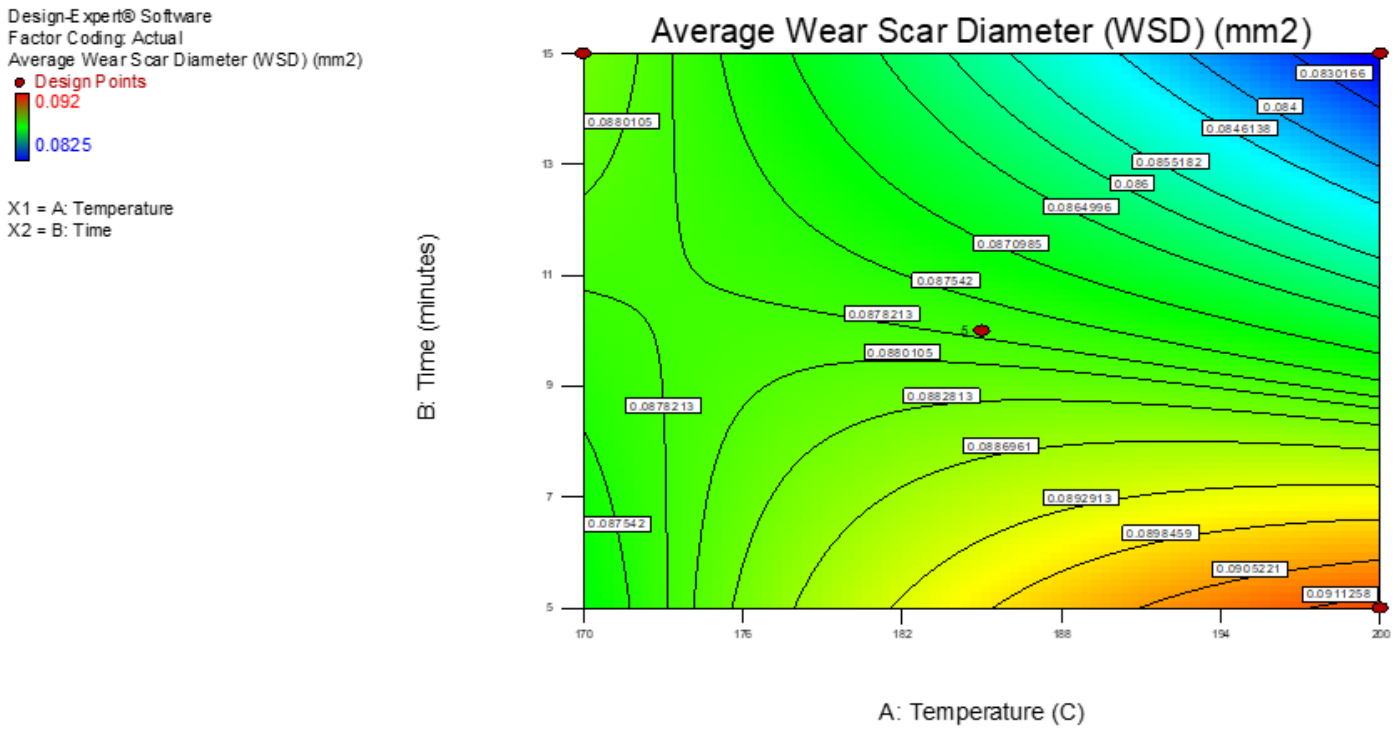


## Figure 9

A contour interaction plot of average WSD for $MoS_2$ nanolubricants

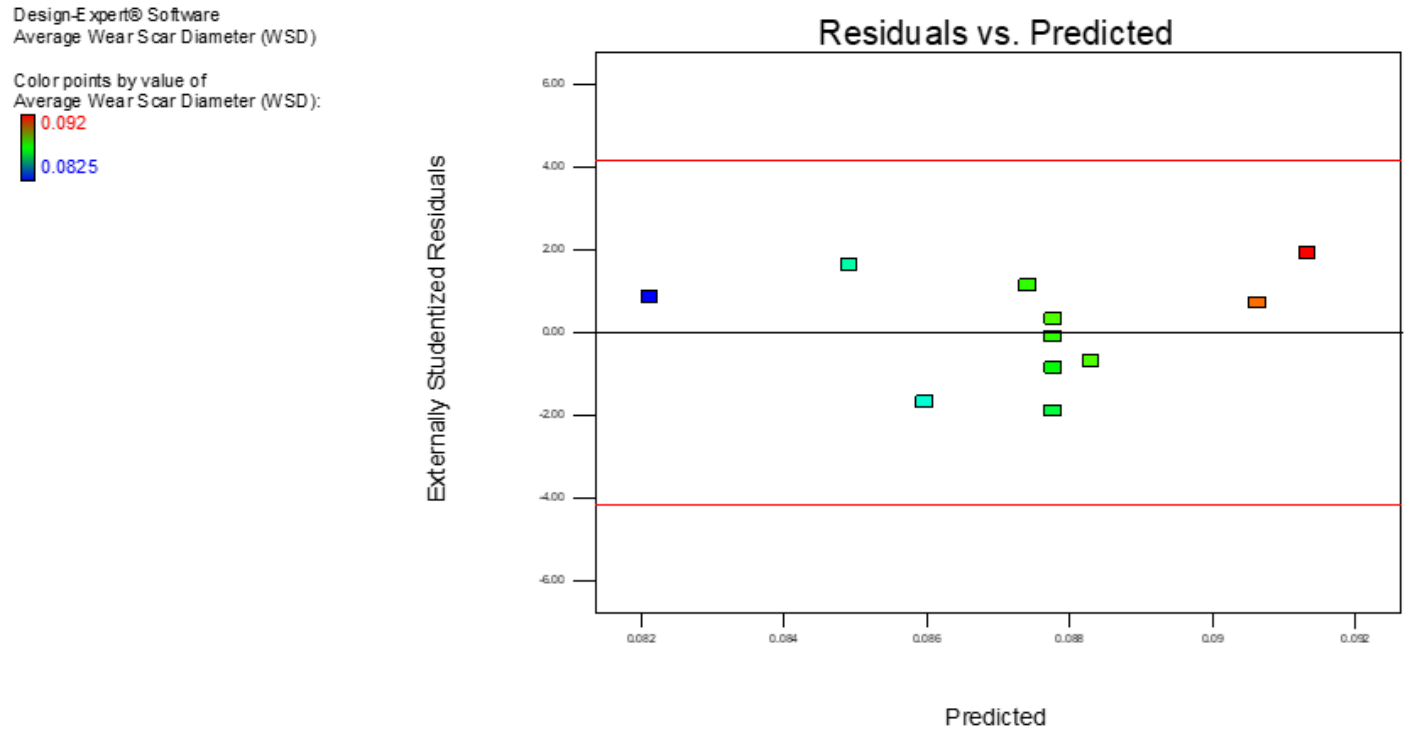


## Figure 10

Residuals vs. predicted of average WSD for $MoS_2$ nanolubricants

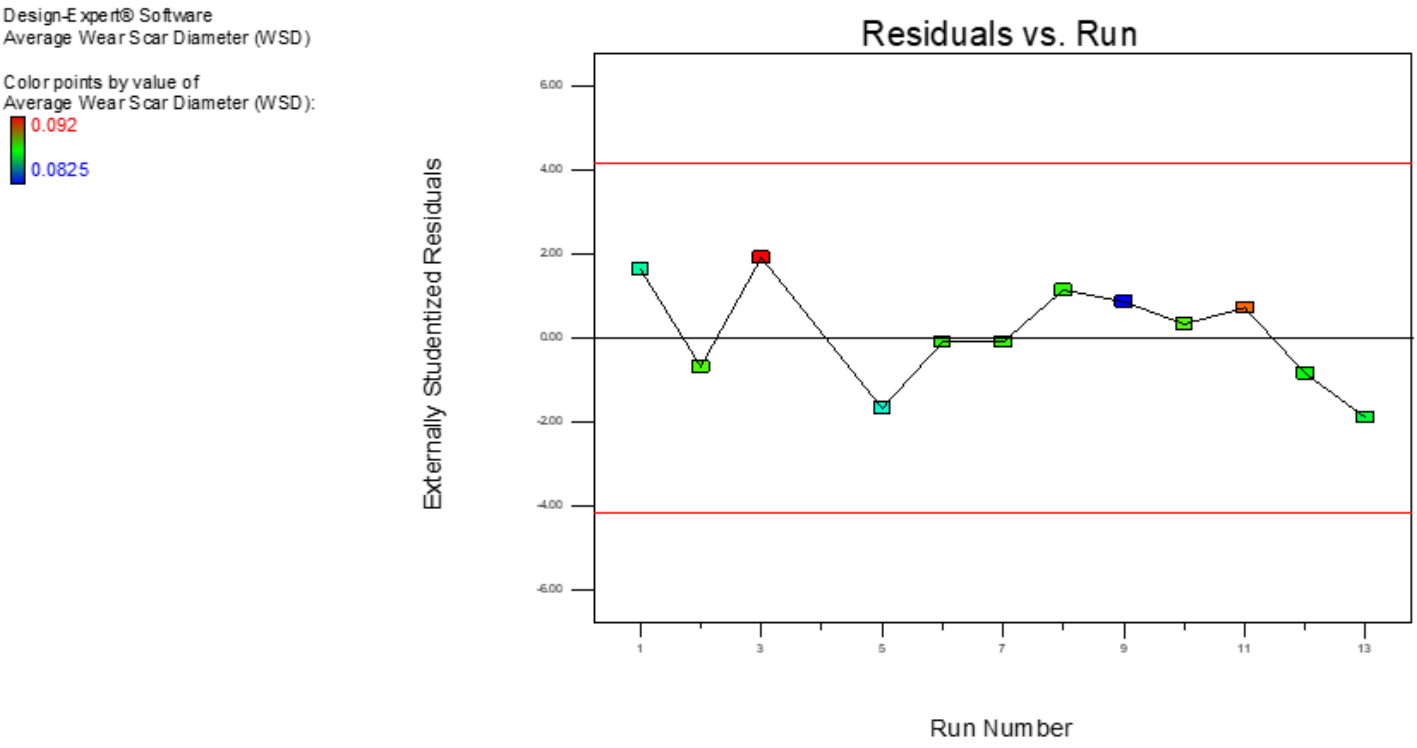


**Figure 11**

Residuals vs. Experimental run of average WSD for $MoS_2$ nanolubricants

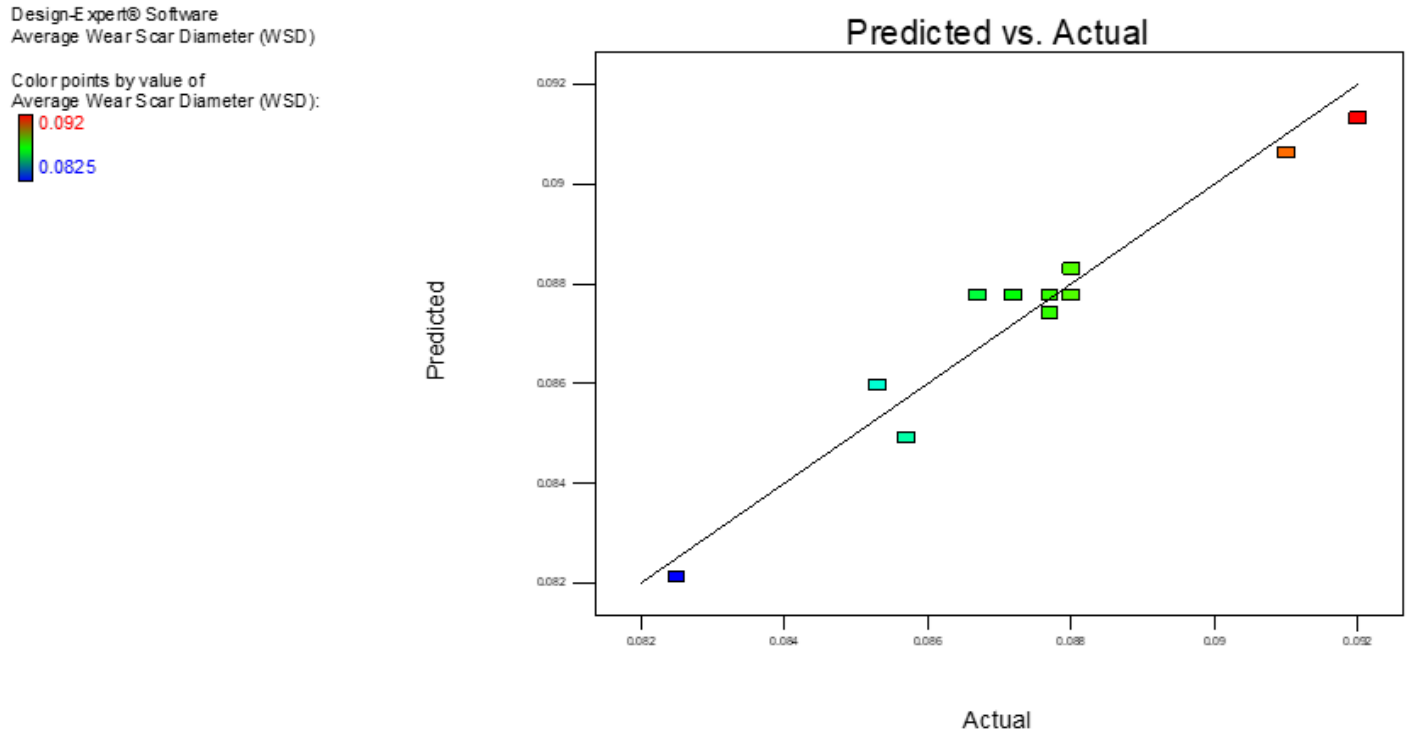

Figure 12

Residuals vs. Experimental run of average WSD for MoS2 nanolubricants

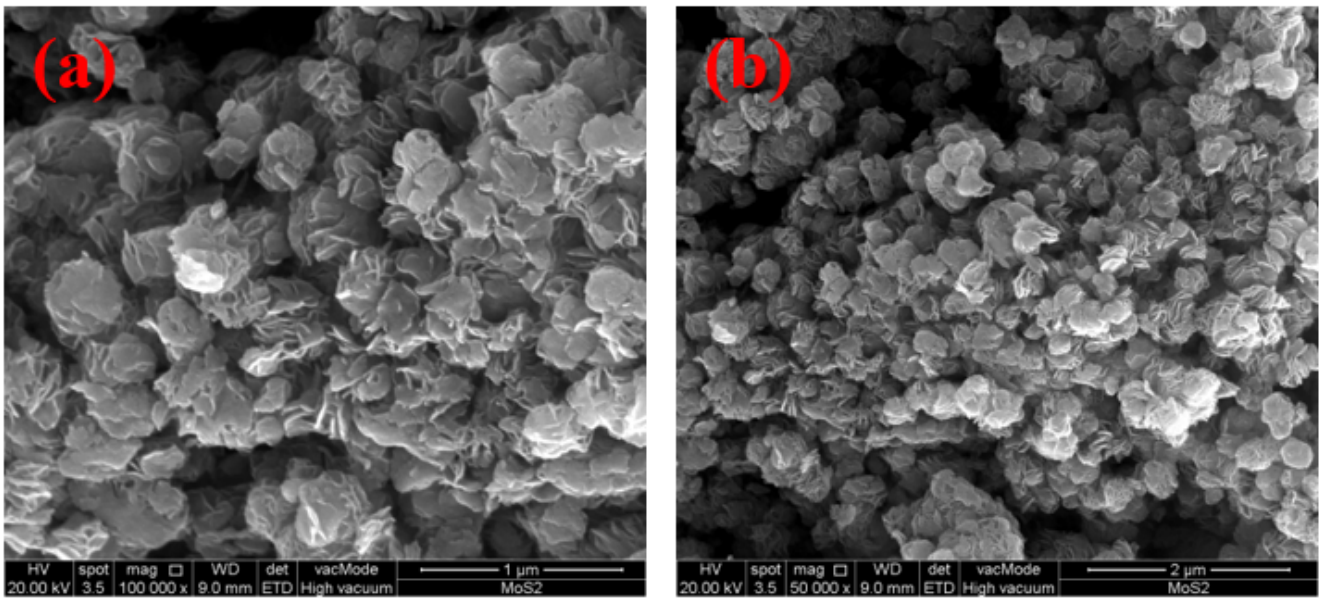


(c)

| ELEMENT | WEIGHT % | ATOMIC % |
|---|---|---|
| S | 38.04 | 64.75 |
| Mo | 61.96 | 32.25 |
| TOTAL | 100 | 100 |

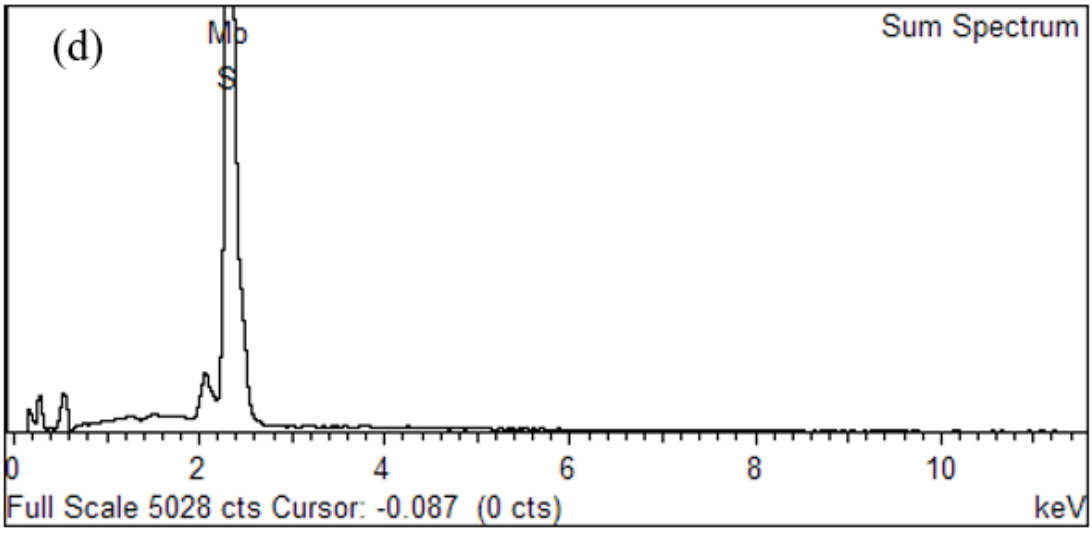


Figure 13

The $MoS_2$ nanoparticles. (a) & (b) FESEM of $MoS_2$ nanoparticles at 2 magnification levels (c) Composition of $MoS_2$ nanoparticles (d) EDS spectrum of $MoS_2$ nanoparticles

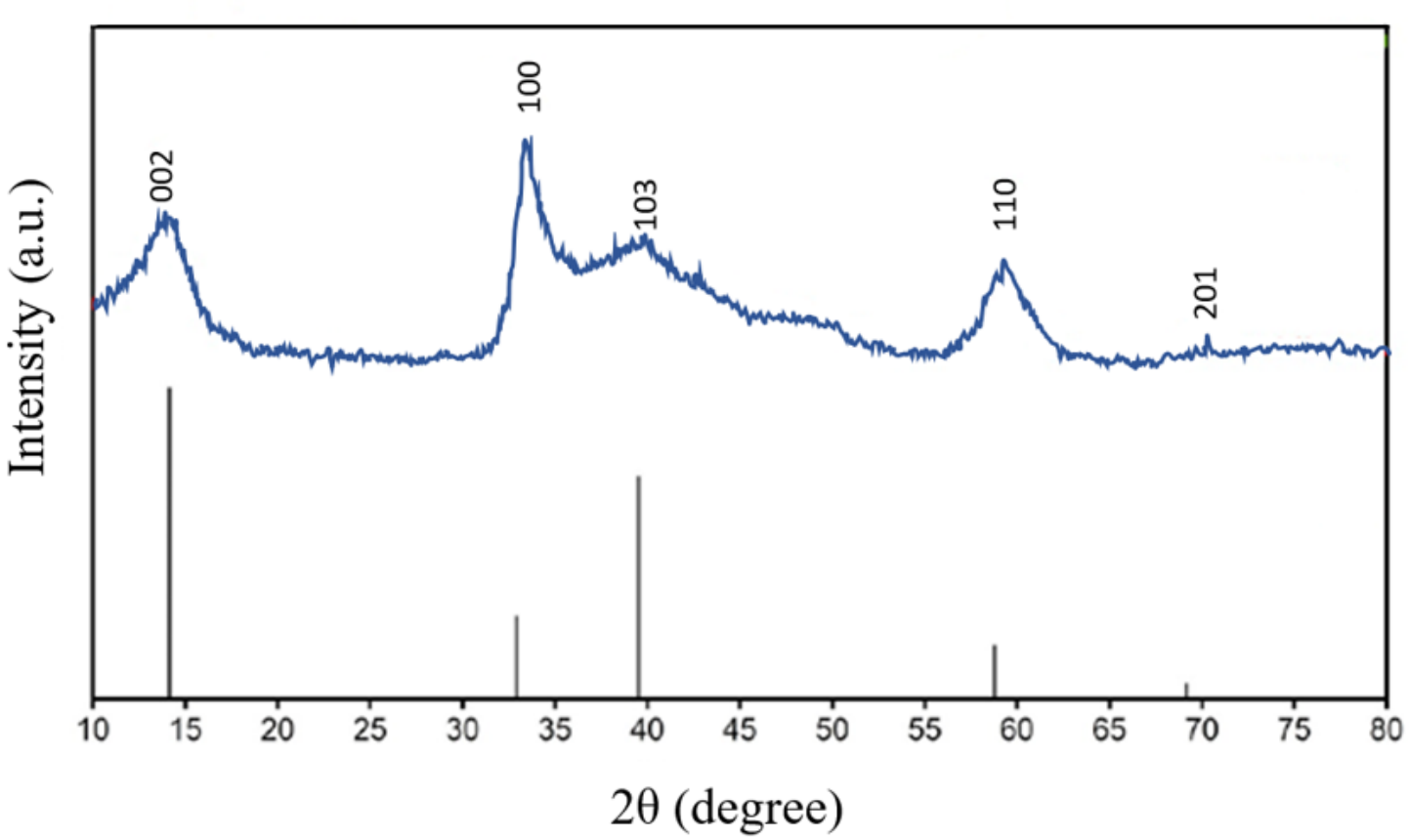


**Figure 14**

XRD pattern of $MoS_2$ nanoparticles

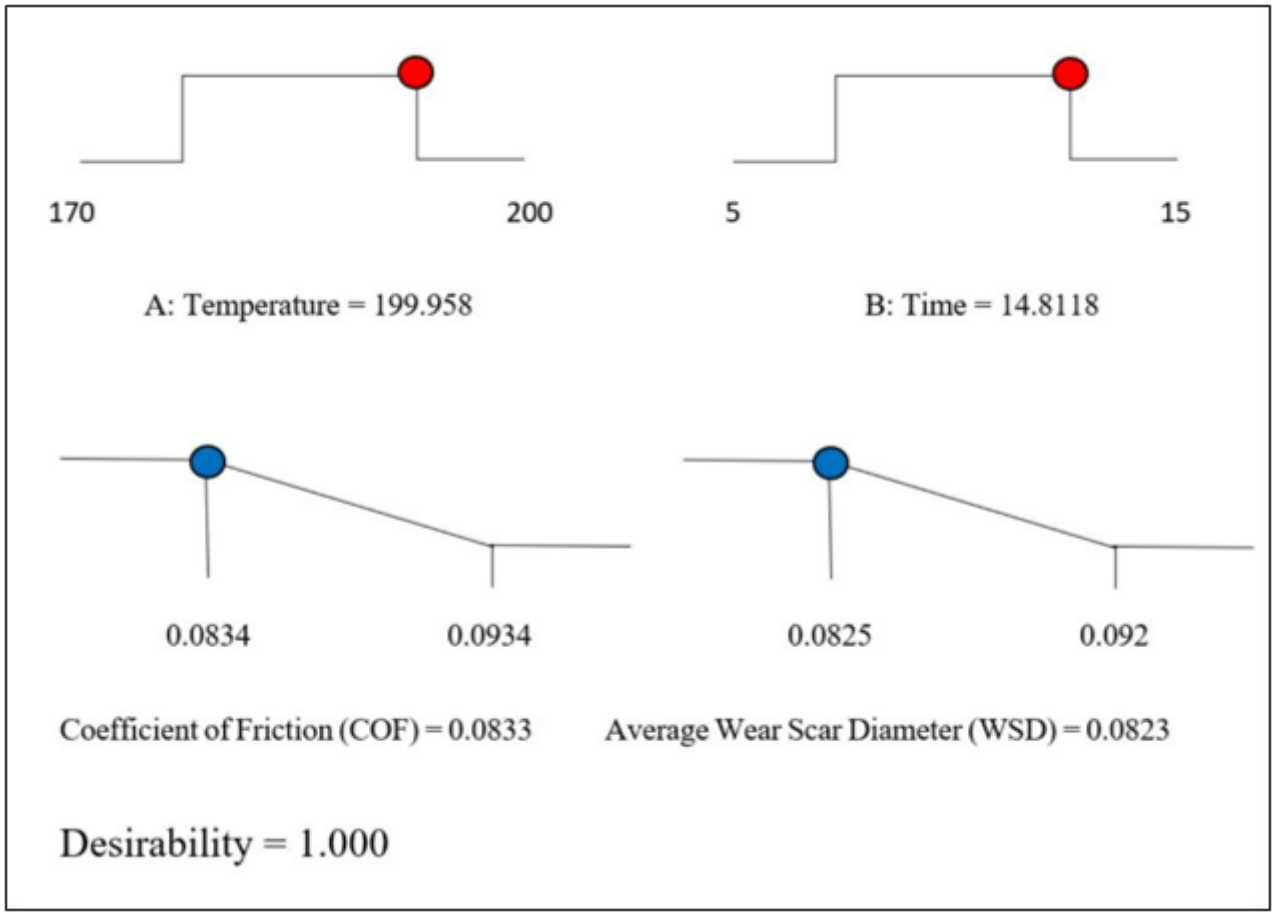


## Figure 15

Ramp function plot for the optimisation of MoS2 nanolubricants

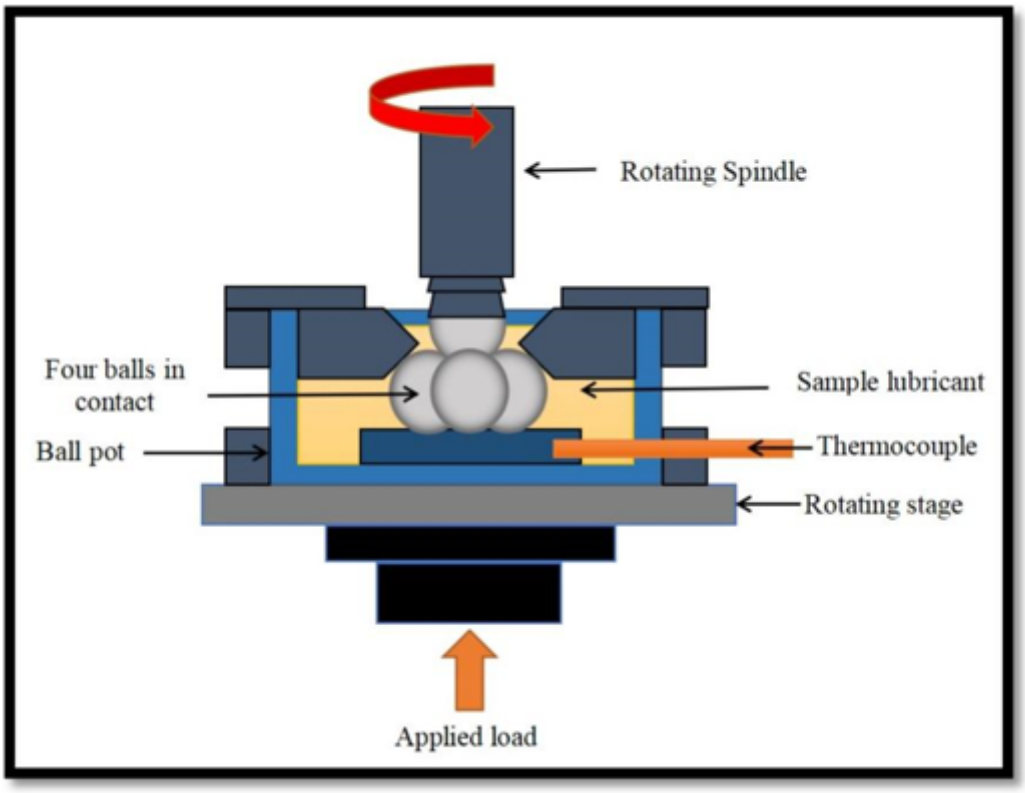


## Figure 16

The experimental configuration of the four ball tribotesters schematic drawing